**Rocznik Ochrona Środowiska**

Volume 26 Year 2024 ISSN 2720-7501 pp. 115-127

https://doi.org/10.54740/ros.2024.012 open access

Received: January 2024 Accepted: March 2024 Published: April 2024

# Effect of Heating Surface Geometry on the Droplets Evaporation under Leidenfrost Conditions

*Tadeusz Orzechowski[1], Sylwia Wciślik[2*]*

[1]*Faculty of Environmental Engineering, Geodesy and Renewable Energy, Kielce University of Technology, Poland*

*https://orcid.org/0000-0002-1727-8186*

[2]*Faculty of Environmental Engineering, Geodesy and Renewable Energy, Kielce University of Technology, Poland*

*https://orcid.org/0000-0003-2152-9686*

[*]*corresponding author's e-mail: sylwiazw@tu.kielce.pl*

**Abstract.** Physical and geometric factors are generally regarded as the main cause of evaporation characteristics of the Leidenfrost droplets levitating above the hot surface. It is well-known and generally accepted that similar research is conducted under different conditions and on individual measurement set-ups. This is one of the potential reasons for the differences in the results of thermal fluxes and computational models in scientific papers. This paper discusses the influence of the heating surface geometry on the heat transfer coefficient $h$ during water drops evaporation under film boiling regime. The variable geometry parameters are the curvature radius of the heating bowl of $R$ = 64 and 254 mm. Individually compiled test stands made it possible to measure the instantaneous drop mass for each $R$ radius and to determine the coefficient $h$. The methodology was validated by calculating the relative error. It changes with the curvature radius and the droplet size, and for droplet mass from about 2 g to 0.3 g does not exceed ±10%. The heat transfer coefficient $h$ is about 15% higher for a drop located on a surface with a larger radius of curvature. Moreover, the method that was devised allows us to estimate the $h$ value for asymmetric droplet shapes. The advantage of the adopted method of measuring the drop mass over time is the possibility of analyzing heat transfer processes in any drop shape range, even in the case of asymmetric ones. Previous research methods were mainly based on determining the mass of the drop by calculating its volume.

**Keywords:** Leidenfrost, film boiling, droplet evaporation, droplet shapes, instabilities formatting

## 1. Introduction

The levitating of droplets above a hot surface has been known since 1756, and like the minimum temperature above which it floats, is called the Leidenfrost phenomenon and temperature, respectively (Leidenfrost 1966). On the other hand, its wide interest is related to the development of cooling technology, fuel evaporation, metal technology processes, and evaporative cooling, as well as in medicine and others (Agrawal et al. 2019, Dupeux et al. 2013, Chen & Huang 2009, Orman & Chatys 2011, Carsky et al. 2022). Depending on the needs, the aim is to maximize the heat flux removed (Breitenbach et al. 2018), especially during emergency operation of, e.g. a nuclear reactor or a highly loaded electronic system, and sometimes only to the desired reduction of the surface temperature, e.g. of the skin during medical treatments. In many technical applications, it is desirable to control the temperature of the material and the discharged heat flux in such a way as not to damage its structure or mechanical properties (Kossakowski et al. 2019).

It is very difficult in systems with a surface temperature higher than the Leidenfrost point. This is due to the highly complex physical nature of the phenomenon. Among others, it is difficult to accurately and unambiguously give the minimum surface temperature at which the beginning of a stable film boiling is observed (Cai et al. 2019). Various values of this point are quoted in the literature (Baumeister et al. 1966). According to (Baumeister et al. (1977), it is a function of surface parameters such as roughness, thermal diffusivity, and environmental parameters. It also describes the evolution of the shape of the evaporating droplet, which can be divided into five categories, presented in Fig. 1.

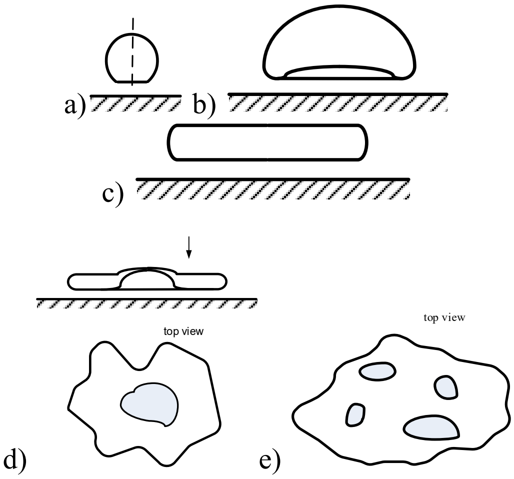


**Fig. 1.** Characteristic shapes of droplets according to (Baumeister et al. 1966); a) a small spherical droplet, b) a large droplet in the form of an almost flat disk, c) a droplet of an extended flat disk and almost constant thickness, d) a droplet of a similar shape as in c) with a single vapor bubble under its surface, e) a very large droplet (puddle) with a few vapor bubbles

Additionally, a very large variety of shapes is observed, taken by the drop floating above the hot surface. Their photographic documentation illustrating individually conducted research can be found in many publications, including (Li et al. 2023, Paul et al. 2015, Ma et al. 2017, Baumeister & Hummil 1965) and many others.

The final goal of research on the nature of the Leidenfrost phenomenon is to determine the amount of heat exchanged, which is the sum of the convective, conduction, radiation, and diffusion flux. Due to the complexity of such issues, given by various researchers, the results are obtained under strong simplifying assumptions. They relate in particular, to the drop's interaction method with the heating surface and the droplet geometry.

Assuming a flat disc-shaped drop floating on a vapour cushion of constant thickness (see Fig. 1b), the expression for the flux of the evaporated mass and the heat transfer coefficient can be given (Baumeister & Humill 1965).

From the literature review, e.g. (Poniewski & Staniszewski 1981, Bernardin & Mudawar 1999), and others, it is shown that the values of Leidenfrost's temperature and also of the heat flux, given by various authors differ significantly, and the reported dependencies often do not correlate together. The reason is the different conditions of measurements carried out on surfaces made of different materials and with different morphologies (Erkan 2019).

Under Leidefrost conditions, a thin vapour layer is deposited beneath the droplet located on the heating base. Vapour thickness varies with the drop size (Ma et al. 2017, Burton et al. 2012). Accordingly, the highest rate in the discharged heat flux is that from the lower surface of the droplet. For larger droplets, residual vapor bubbles appear, the volume of which is comparable to the volume of the liquid phase (Snoeijer 2009). Many experimental studies discuss the heat and mass transfer phenomena that occur in the vapour layer under the drop (Pastuszko et al. 2021, Roques-Carmes 2018). The papers and research describe the evaporation of liquids by the mass, momentum, and energy balance. Due to computational difficulties, the presented calculations often have very small axially symmetrical droplet geometry (Chen & Bertola 2016). For instance, in (Drachal & Poniewski 1981) the calculations were performed for droplets as shown in Fig. 1a; they are shaped as the sphere truncated at the bottom. The results were compared with the evaporation measurements with an initial volume of $43.292 \cdot 10^{-9}$ $m^3$ (i.e. approx. 0.043 g). Such an assumption seems to be proper and justifies the adopted droplet geometry as in Fig. 1a, although the bottom surface is not flat in reality.

As already mentioned, larger drops are subject to various types of fluctuations. They may result from thermal forces related to the minimum energy necessary to induce oscillatory motion (Baumaister et al. 1977). In (Poniewski & Staniszewski, 1986), the value of the local potential was adopted as a measure of energy dissipation. There were also numerical calculations of the vapour film thickness under the drop and the minimum film boiling point value as a function of pressure. The results obtained are in good correlation with values available in the literature. They are also confirmed by photographic documentation illustrating the interaction of the liquid phase with the heating surface (Wciślik & Mukherjee 2022, Pavlenko 2005).

The behaviour of a droplet floating above a hot surface is stochastic. In such papers, a statistical analysis was usually performed to determine droplets evaporation times. The results obtained for water droplets were compared with the experimental values, confirming their good compliance. It is worth adding that the statistical analysis is not always confirmed in further research, an example of which is the paper (Orzechowski & Poniewski 1996).

Measurements of the evaporating droplet are usually carried out based on photographic documentation. In the papers cited above, no more than two cameras are used, one is placed above the drop, and the other observes its lateral surface. On this basis, it is possible to calculate the volume, and thus the mass, of only axisymmetric objects, which under real conditions can only concern small droplets, as shown in Fig. 1a. Larger volume droplets oscillate, making their shapes highly irregular and stochastic.

An additional limitation is the so-called chimney effect. It is associated with the deposition of large vapour bubbles and their irregular release. In such cases, it is not possible to properly calculate the droplet volume. The paper (Orzechowski & Wciślik 2012) proposed placing a measuring stand on a scale, the RS 232 port of which was programmed to record mass indications continuously on a computer disk. The limitation of the proposed method of measurement is the scale accuracy. It means that the research carried out according to this methodology has a lower limit and does not include droplets in the range 'a' according to Fig. 1. An example of good accuracy results is the paper (Orzechowski 2021), in which the heat is dissipated from the drops weighing from about 2.5 g to only about 0.3 g.

The evaporation process of droplets levitating above the hot surface is a function of physical and geometric parameters. The research is carried out in various conditions and on individually designed measuring stands. This is one reason for the discrepancy in the heat flux results and computational models available in the literature. One of the variable parameters is the geometry of the heating surface.

The main subject of the presented research is the geometry of the heating surface's influence on the amount of heat dissipated during cooling, which is an example of a levitating droplet of water in the Leidenfrost regime. For this purpose, a research stand with a different heating surface shape was built. One refers to R = 254 mm curvature radius, and the other of R = 64 mm. In this way, it was proven how surface/geometric conditions affect the heat transfer coefficient and what errors are related. Moreover, a correlation relationship for determining the mass of an evaporating liquid drop depending on its initial diameter was provided along with validation.

## 2. Experimental Facility

The main research goal is measuring mass and registering the horizontal projection of an evaporating droplet onto the heating surface.

### 2.1. Limitations

An electronic scale with high accuracy and one order of lower sensitivity, amounting to 0.2 g and 0.001 g, respectively, was used to register the constantly changing drop mass. The device has a factory-built RS232 interface for communication with a computer and requires dedicated software. The technical conditions of the device made it possible to measure instantaneous values of indications with a maximum frequency of 5 Hz. An important feature of such measurement organization is remote and non-contact control of starting measurements, balancing, recording frequency, etc. However, the basic limitation of the scale, which must be considered, is its measuring range of up to 500 g. It required a particularly careful construction of the test stand.

### 2.2. Heating surface

The basic research module is a copper cylinder on which a band heater. Its power must be sufficient to stabilize the surface temperature, i.e. up to 500°C. As shown in Fig. 2, a K-type thermocouple is centrally located beneath the heating cylinder; the indications of the K element are used to control the temperature of the heating surface.

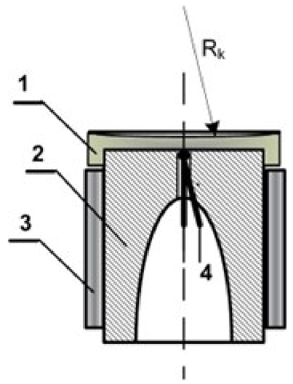


**Fig. 2.** Copper heating cylinder: 1 – copper cover with a surface with a radius of curvature $R_k$, 2 – copper cylinder, 3 – band heater, 4 – thermocouple

The upper surface of the copper cover of the cylinder is shaped like a bowl with a very large radius of curvature. This enables a centric and stable position of the tested liquid drop. A heater was mounted on the outer surface and fed electricity through freely suspended wires. Due to the potential influence of the cable elasticity on the scale readings, the stand must be conditioned for several hours. Detailed descriptions of the measurement procedure and the stand are provided in (Orzechowski & Wciślik 2012, Orzechowski 2021).

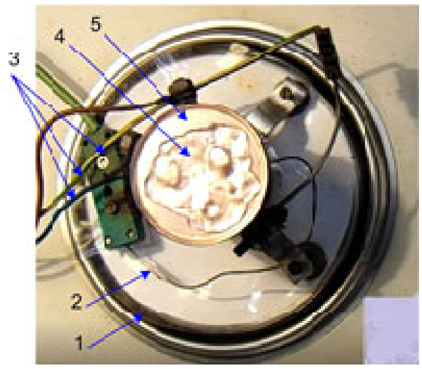


**Fig. 3.** Photograph of the experimental set-up (top view): 1 – scale, 2 – thermocouple, 3 – electrical power supply, 4 – droplet, 5 – copper cover

### 2.3. Drop generation

The shape of the large drops is usually highly irregular in nature, as shown in Figs. 1b to 1e. Moreover, it changes over time. In such cases, the estimation of the volume of the drops, and thus their mass – based on photographs recorded with cameras placed, for example, only in two planes, i.e. the top and the side – fails. However, the drop horizontal projection on the heating surface may be calculated with sufficient accuracy when appropriate software is used for the analysis of photos taken sequentially or a film recorded by a camera placed above the droplet. Fig. 3 shows the test stand top photographed with a visible irregular drop of liquid, under which three bubbles are located. This is an illustration of the shape shown in Fig. 1e.

### 2.4. Mass measurements

Placing a drop on the scale always slightly interferes with its indications. For this reason, the analysis of the performed measurements was carried out after its readings stabilized. In the presented research, it was waited until the drop mass was about 2 g. The control program for collecting and recording measurement data assumed a constant frequency equal to 1 Hz. With the increase of time, when the drop mass is only a few times greater than the balance accuracy, the relative error grows quickly, and the results are burdened with a large error (Snoeijer & Brunet 2009). Due to this, this range of droplet lifetime is not analyzed in these studies.

## 3. Results and Discussion

The results of the experiments are presented in Fig. 4, which shows the mass loss curve for different droplet mass and heating surface geometry of R = 254 mm. The average value of surface temperature was $T_w$ = 390±2°C.

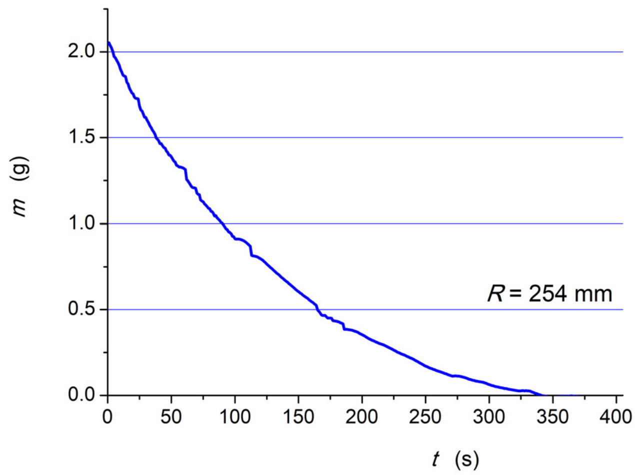


**Fig. 4.** Evaporation of the water droplet from the heating base with a radius of curvature R = 254 mm

### 3.1. The effect of droplet size

In the case of large-mass drops, various instabilities are observed (see Fig. 5). They arise from complex convection movements inside the droplet and the gas phase deposition under its bottom surface. With large water drops, usually greater than 1 g, there are bubbles that grow and release to the outside. The deviations of the scale indications are visible in Fig. 4. They disappear with time and decrease in the drop mass, as can be seen in Fig. 6. The figure displays the area of the drop perpendicular projection onto the heating surface as a function of its mass $A(m)$. It is worth noting that this is a roughly linear relationship.

**Fig. 5.** Instabilities during evaporation of the water droplet from the heating base

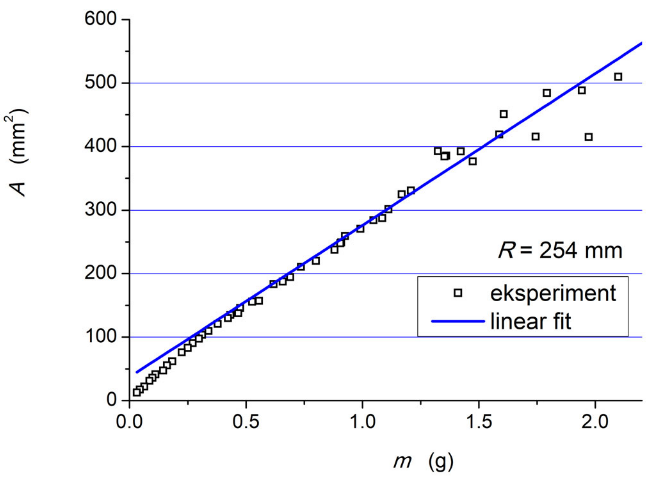


**Fig. 6.** Dependence of the perpendicular projection area of a drop on its mass

Visible deviations from the straight line in Fig. 6 concern large drops when vapour bubbles are released and very small ones with a mass below 0.3 g. The influence of both disturbances on the accuracy of the measurement can be assessed based on the relative error. Its values are shown in Fig. 7 as a function of mass.

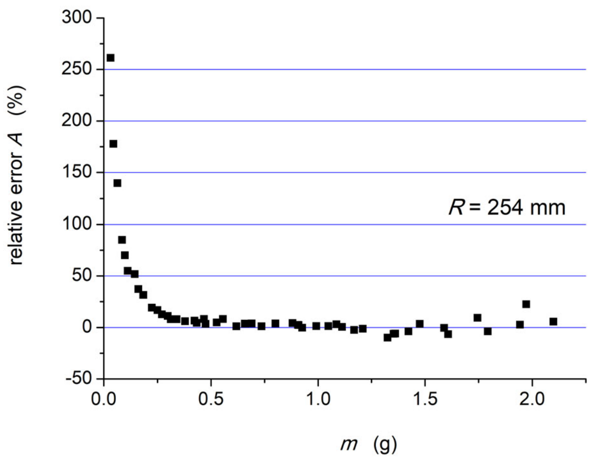


**Fig. 7.** Relative error between the projection area of the drop and the linear relationship as in Fig. 6

In the range of the whole droplet lifetime, when the production of vapour bubbles is observed, i.e. in the case of water, it is usually for m > 1 g, the value of relative error refers to the choice of the moment of the drop perpendicular projection onto the heating base. This area is quite large during the bubble growth and gradually increases over time. After its release, the instantaneous value of this projection is low, which can be seen in Fig. 5. The situation is different in the case of small droplets, where, with a mass of about 0.3 g, this error rapidly increases and in the registered range it reaches several hundred per cent.

Based on the measured values of the perpendicular drop projection area shown in Fig. 6, the equivalent diameter of a circular droplet was calculated according to formula (1), and the results are shown in Fig. 8.

$$D=2\sqrt{(A/\pi)} \tag{1}$$

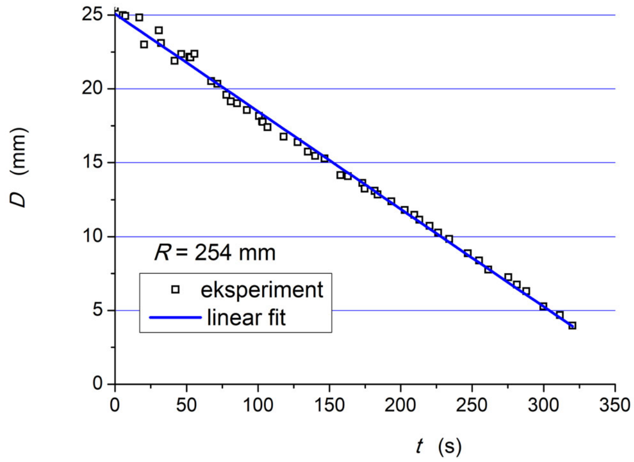


**Fig. 8.** Calculated droplet diameter over time

### 3.2. The effect of the heating surface geometry

The evaporation process of drops levitating above the hot surface depends on many physical and geometric parameters. For this reason, the results reported in the literature often differ quite significantly. One of the reasons is the geometry of the heating surface. The drop lifted on the vapour cushion shows a strong tendency to move. Such uncoordinated movements can be counteracted by designing a heating surface in the form of a bowl with a given radius, R. However, this parameter has a large impact on the test result. Fig. 9 shows two measurements of the change in drop mass over time, performed under the same conditions, that is, at $T_w = 396°C$, but on two copper heating surfaces shaped as a bowl with different curvature radiuses, R: 254 mm and 64 mm, respectively.

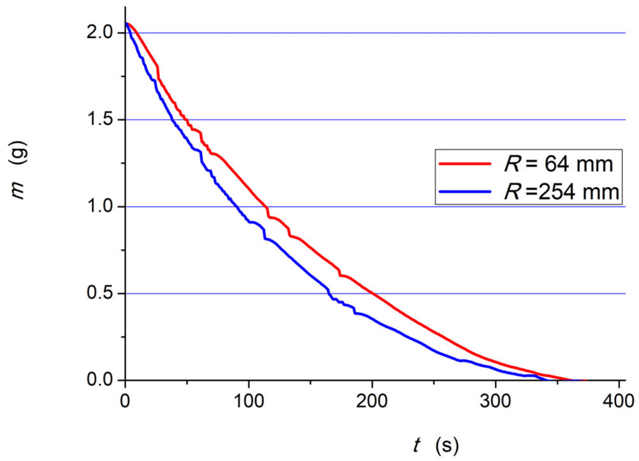


**Fig. 9.** Change in the water droplet mass with time for a constant wall temperature Tw ≈ 390°C and varying curvature radius, R = 64 mm – red line, R = 254 mm – blue line

The drop evaporation time on the radius of a surface with the curvature R = 64 mm is slightly longer than the corresponding time on the surface with a larger radius (see Fig. 9); the difference is several seconds. On the other hand, on a surface with a larger curvature radius, the droplet achieves the same instantaneous mass faster than the corresponding one on the surface of a smaller R. For example, at R = 254 mm, the drop reaches a mass of 1 g after t ~ 90 s, which is approx. 22 s faster than at R = 64 mm. Simultaneously, as shown in Fig. 10, for the same mass, the drop perpendicular projection onto a surface is smaller for R = 254 mm than for R = 64 mm.

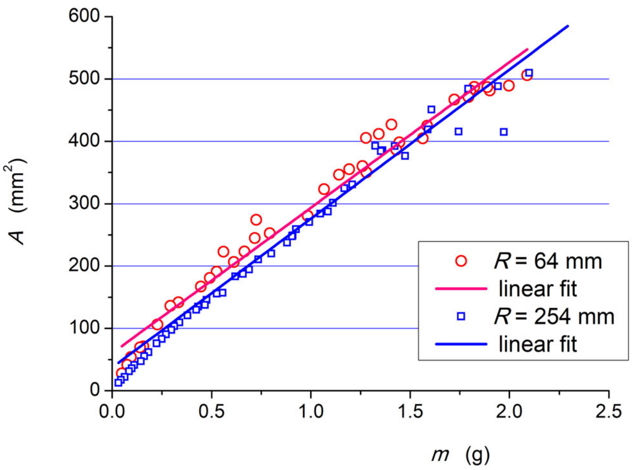


**Fig. 10.** Perpendicular projection areas of drops on their mass (R = 64 mm – red line, R = 254 mm – blue line)

The same applies to the equivalent diameter, D calculated based on the drop surface area and equation (1). Fig. 11 displays that after the same evaporation time, D is greater for a smaller curvature radius and, for example, it amounts to ~17.5 mm for t = 150 s and ~15.0 mm for the same evaporation time and cooper cylinder curvature radius R = 254 mm.

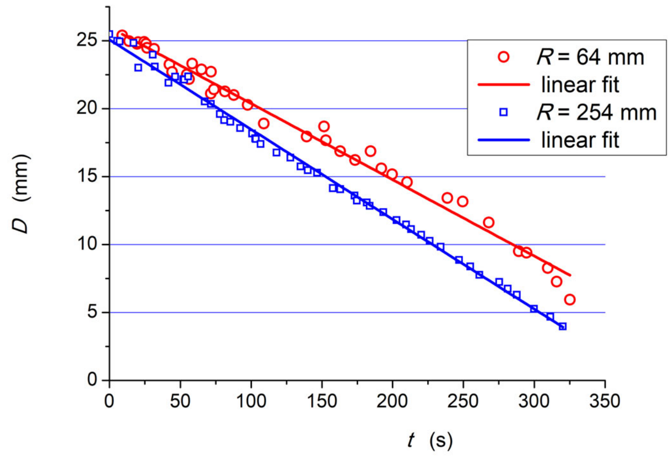


**Fig. 11.** Calculated droplet diameters as a function of time (R = 64 mm – red line, R = 254 mm – blue line)

## 4. Heat Transfer Analysis

The conductivity equation often describes the Leidenfrost phenomenon concerning liquid drop evaporation, which relates mainly to the thin vapour layer under the drop bottom surface. In such conditions, according to the review (Sodtke et al. 2007), conduction heat transfer is dominant, and convection, radiation and diffusion heat transfer can be neglected, but there is insufficient experimental evidence for the correctness of this assumption. In this paper, it is proposed to form a substitute value for the heat transfer coefficient, $h$, which is the sum of the appropriate coefficients, taking into account all mentioned phenomena, $h = h_{cond} + h_{conv} + h_{rad}$.

Such a determined coefficient can be here referred to the drop perpendicular projection onto the heating base and can be used for the following heat and mass transfer balance that describes the drop mass change over time d$t$:

$$\frac{dm}{dt} = -\frac{1}{K} h\,(T_w - T_d)A \tag{2}$$

where $T_w$, $T_d$ are surface and droplet temperatures, respectively, $A$ – the droplet orthogonal projection onto the heating surface, the $K$ parameter is given by the formula:

$$K = \frac{H_{fg} + c_p(T_l - T_d)}{T_w - T_d} \tag{3}$$

where $H_{fg}$ – phase change enthalpy at the saturation temperature, $c_p$ – specific heat at atmospheric pressure and $T_s$ – saturation temperature.

The drop mass $m$ changes linearly with its perpendicular projection on the heating surface $A$ in the range shown in Figs. 6 and 9. The function can be written by the following formula:

$$A = a_A + b_A m \tag{4}$$

where $a_A$ and $b_A$ represent the intercept and the straight-line slope, respectively.

In turn, based on Figs. 8 and 10, the apparent time-changed diameter of the droplet projection can be defined as:

$$D = D_0 - b_D t \tag{5}$$

where $D_0$ is the diameter in the initial moment of evaporation and $b_D$ is the slope of the straight line.

From Equations (2), (3) and (4), the formula for the total heat transfer coefficient can be obtained as:

$$h = \frac{\sqrt{\pi} K b_D}{b_A \sqrt{A}} \tag{6}$$

In the next step, using the equations mentioned above, the formula for droplet mass change over time can be written:

$$m= -\frac{a_A}{b_A} + \frac{1}{b_A}\frac{\pi}{4}D_0^2\left(1 - \frac{t}{D_0/b_D}\right)^2 = -\frac{a_A}{b_A} + \frac{1}{b_A}A_0\left(1 - \frac{t}{t_0}\right)^2 \tag{7}$$

where $t_0$ is the drop lifetime, and $D_0$ is its initial diameter.

Fig. 12 compares the drop mass measured and calculated according to Equation (7), levitating above the surface with a large radius of curvature ($R$ = 254 mm). In the large mass range up to about 0.3 g, a fairly good agreement of the drop mass measurement results with the calculations can be seen. For drops weighing less than 3 g, there are large and quickly increasing differences between the two curves with time.

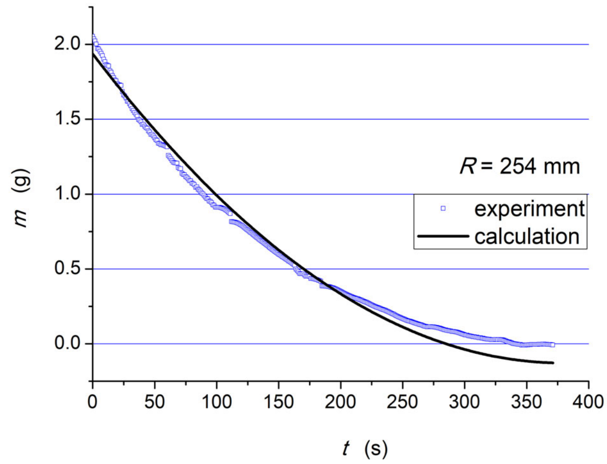


**Fig. 12.** The measured and calculated change in the mass of the drop over time placed on a surface with a radius of curvature of $R$ = 254 mm

Fig. 13 shows the relative error between the measured and calculated change in drop mass versus time. This error increases sharply for droplets weighing less than 0.3 g. Analogous graphs for a droplet floating above a surface with a small radius of curvature ($R$ = 64 mm) are shown in Figs. 14 and 15, respectively. In both cases, large and increasing errors are observed for small droplets. However, the relative error in the droplet mass from about 2 g to 0.3 g does not exceed ±10%.

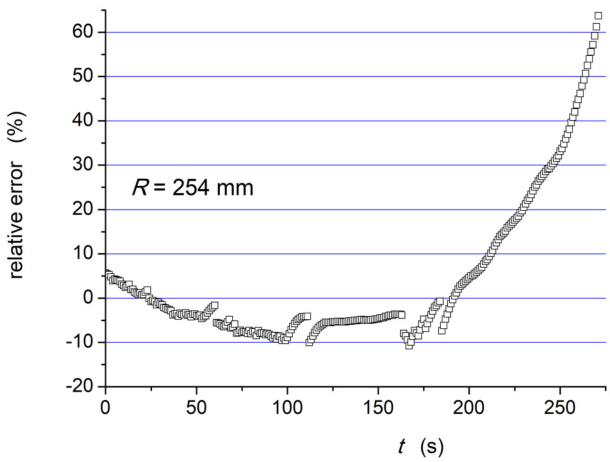


**Fig. 13.** Relative error between the lines in Fig. 12

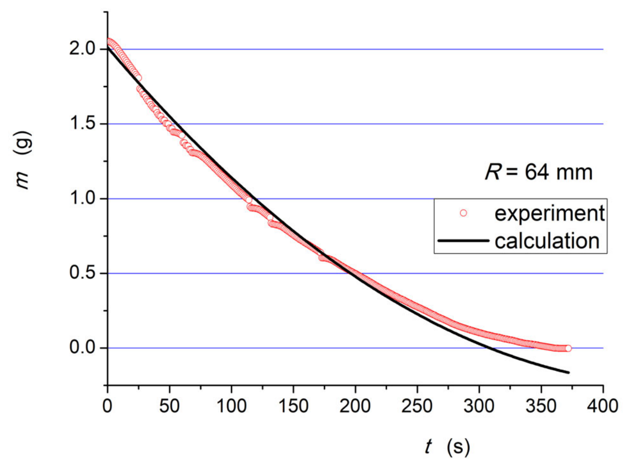


**Fig. 14.** Drop mass changes with time, levitating over a surface with a radius of curvature of $R$ = 64 mm

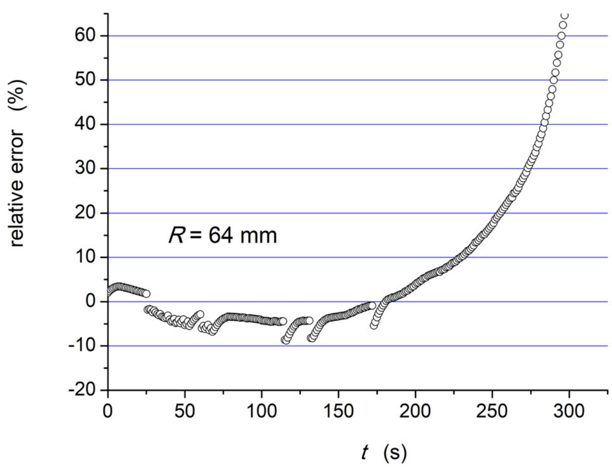


**Fig. 15.** Relative error between the lines in Fig. 14

The relative error (shown in Figures 13 and 15) between the measured and calculated values of droplet mass loss as a function of its lifetime (for different radii of curvature) seems important from the proposed correlation (Equ. 7) point of view.

The discontinuity of the error function results from the fact that for large droplets, usually weighing more than 1 g, there is an intense production of vapour lying under the bottom surface, which, when accumulated large enough, rapidly escapes in the form of bubbles. This first causes a relatively slow increase in the droplet surface, then its rapid decrease after the excess gas phase is released. Such phenomena directly cause deviations from the linear relationship, $A(m)$, shown in Figure 6. Such deviations are also characteristic of very small droplets, i.e. with a mass below 0.3 g, when, with decreasing mass, the drop tends to become spherical.

The slope values of the $b_A$ and $b_D$ lines are shown in Figs. 10 and 11, respectively, determine the local value of the heat transfer coefficient, $h$. Its values for both surfaces are shown in Fig. 16. It is about 15% higher for a drop located on a surface with a larger radius of curvature. In both cases, its value increases rapidly with the drop in droplet mass, while the growth becomes steadier for droplets with a mass below 0.2 g.

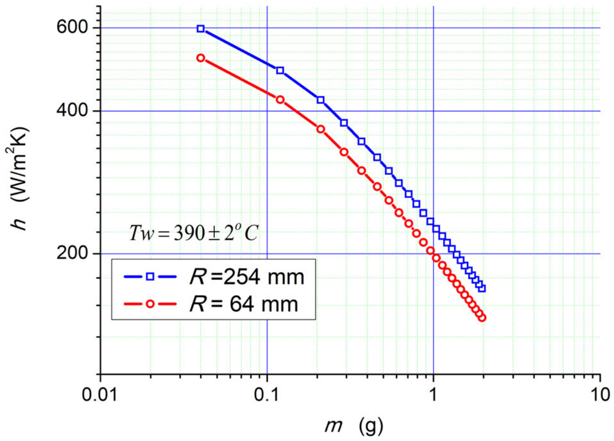


**Fig. 16.** Heat transfer coefficient as a function of the droplet mass for surfaces with different radii of curvature

## 5. Conclusions

Designing the course of the technological process, in which maintaining the proper cooling rate of the hot surface is one of the parameters, requires possibly precise specification of the dependencies determining the amount of heat flux removed. This is especially difficult in the phase change processes, for which the relationships reported in the literature often differ significantly. This also applies to the evaporation of liquid droplets from the hot surface, including its film boiling.

The method proposed here is based on direct measures of the drop mass during its evaporation. On this basis, the total heat transfer coefficient *h* is calculated with good precision, true for the 1b to 2e ranges in Fig. 1 (Orzechowski 2021, Orzechowski & Wciślik 2014). This improves engineering heat transfer calculations when the Leidenfrost effect accompanies cooling. Moreover, the results confirm the previous findings that the heat transfer coefficient increases with the droplet size and the heating surface curvature. One of the parameters not described in the literature is the shape of the heating surface. Therefore, the influence of the shape of the heating base on the amount of dissipated heat flux is investigated here. For this purpose, two radii of curvature of the heating surface are analyzed, amounting to 64 and 254 mm, respectively. It was found that in the range of linear dependencies of the perpendicular projection on the heating surface as a function of mass and the equivalent drop diameter as a function of time, the calculated heat transfer coefficient is about 15% higher for a drop of water located on the surface with a larger radius of curvature. The influence of the shape of the heating surface on the amount of heat flux carried away by the large drops floating above the surface with a temperature above the Leidenfrost point is significant.

Measurements of the droplet volume, and thus its mass, based on photographic documentation, are acceptable only for axisymmetric shapes. For droplets maintained in the Leidenfrost regime, such forms are stable only at their very small dimensions. The advantage of the adopted method of measuring the mass over time is the possibility of analyzing heat transfer processes in any drop shape range, even in the case of asymmetric ones. The only limitation is the accuracy of the scale used. In the presented research, the linear dependence of the drop mass on its perpendicular projection on the heating surface and the diameter of the droplet in time was used. For droplets with a mass greater than 3 g, the relative error was always less than 10%. On the other hand, this error grows sharply for $m < 3$ g, which in the presented research made it impossible to analyze this range of heat transfer.

Future research and potential applications of the study mainly concern using other fluids with energetic potential than water, e.g. nanofluids or refrigerants.

*Sylwia Wciślik thanks to Ph.D. hab. eng. Tadeusz Orzechowski for conceptualization, validation and professional, scientific support while writing this paper.*
*The project is supported by the program of the Minister of Science and Higher Education under the name: 'Regional Initiative of Excellence' in 2019-2023 project number 025/RID/2018/19 financing amount PLN 12,000,000.*

## References


Agrawal, P., Wells, G.G., Ledesma-Aguilar, R., McHale, G., Buchoux, A., Stokes, A., Sefiane, K.A. (2019). Leidenfrost heat engine: sustained rotation of levitating rotors on turbine-inspired substrates. *Appl. Energy*, *240*, 399-408. https://doi.org/10.1016/j.apenergy.2019.02.034

Baumeister, K.J., Humill, T. (1965). *Creeping flow solution of the Leidenfrost phenomen*. NASA TN D-3133.

Baumeister, K.J., Hendricks, R.C., Hamill, T.D. (1966). *Metastable Leidenfrost states*. NASA TN D-3226.

Baumeister, K.J., Hendricks, R.C., Schoessow, G.J. (1977). *Thermally driven oscillations and wave motion of a liquid drop*. National Heat Transfer Conference, Salt Lake City, Utah, August 14-17. NASA TM X-73625.

Bernardin, J.D. Mudawar, L. (1999). The Leidenfrost point: experimental study and assessment of existing models. *ASME J Heat Transf.*, *121*, 884-903. https://doi.org/10.1115/1.2826080

Breitenbach, J., Roisman, I.V., Tropea, C. (2018). From drop impact physics to spray cooling models: a critical review. *Exp Fluids*, *59*(55). https://doi.org/10.1007/s00348-018-2514-3

Burton, J.C., Sharpe, A.L., van der Veen, R.C.A., Franco, A., Nagel, S. R. (2012). Geometry of the Vapor Layer Under a Leidenfrost Drop. *Phys. Rev. Lett.*, *109*, 074301. https://doi.org/10.1103/PhysRevLett.109.074301

Cai, Ch., Mudawar, I., Liu, H., Si, Ch. (2020). Theoretical Leidenfrost point (LFP) model for sessile droplet. *International Journal of Heat and Mass Transfer*, *146*, 118802, ISSN 0017-9310. https://doi.org/10.1016/j.ijheatmasstransfer.2019.118802

Chen, S.M., Bertola, V. (2016). Jumps, somersaults, and symmetry breaking in Leidenfrost drops. *Phys. Rev. E*, *94*, 021102. https://doi.org/10.1103/PhysRevE.94.021102

Chen, RH., Huang, YL. (2009). Collision of a liquid drop on the edge region of a plate heated above the Leidenfrost temperature. *Exp Fluids*, *47*, 223-237. https://doi.org/10.1007/s00348-009-0652-3

Dupeux, G., Baier, T., Bacot, V., Hardt, S., Clanet, C., Quéré, D. (2013). Self-propelling uneven Leidenfrost solids. *Phys. Fluids*, *25*, 1-7. https://doi.org/10.1063/1.4807007

Drachal, A., Poniewski, M. (1981). *Przepływ pary i ciepła w poduszce parowej pod kroplą cieczy we wrzeniu błonowym*. Materiały XI Zjazdu Termodynamików, Szczecin-Świnoujście, cz. 1, 84-81. (in Polish)

Erkan, N. (2019). Full-field spreading velocity measurement inside droplets impinging on a dry solid-heated surface. *Exp Fluids*, *60*, 88. https://doi.org/10.1007/s00348-019-2735-0

Kaniowski, R. (2023). Pool Boiling of Novec-649 on Inclined Microchannel. *Energies*, *16*(5), 2476. https://doi.org/10.3390/en16052476

Kossakowski, P. G., Wciślik, W., Bakalarz, M. (2019). Effect of selected friction stir welding parameters on mechanical properties of joints. *Archives of Civil Engineering*, *65*(4), 51-62. https://doi.org/10.2478/ace-2019-0046

Leidenfrost, J.G. (1966). On the fixation of water in diverse fire. *International Journal of Heat and Mass Transfer*, *9*(11), 1153-1166.

Li, A., Li, H., Lyu, S. et al. (2023). Tailoring vapor film beneath a Leidenfrost drop. *Nat Commun*, *14*, 2646. https://doi.org/10.1038/s41467-023-38366-z

Ma, X., Liétor-Santos, J.J., Burton, J.C. (2017). Star-shaped oscillations of Leidenfrost drops. *Physical Review Fluids*, *2*, 031602, 1-8. https://doi.org/10.1103/PhysRevFluids.2.031602

Orman, Ł.J., Chatys, R. (2011). *Heat transfer augmentation possibility for vehicle heat exchangers*. Proc. of 15$^{th}$ Int. Conf. "TRANSPORT MEANS" (Kaunas, Lithuania), 9-12.

Carsky, M., Solcova, O., Soukup, K., Kralik, T., Vavrova, K., Janota, L., Vitek, M., Honus, S., Jadlovec, M., Wimmerova, L. (2022). Techno-Economic Analysis of Fluidized Bed Combustion of a Mixed Fuel from Sewage and Paper Mill Sludge. *Energies*, *15*(23), 8964. https://doi.org/10.3390/en15238964

Orzechowski, T., Poniewski, M. (1996). *Natural Convection inside the Evaporating Droplet – Preliminary Experimental Investigation*. Int. Conf. on Heat Transfer with Change of Phase, Kielce, Vol. II, 125-137, PL ISSN 0239-4979.

Orzechowski, T., Wciślik, S. (2012). *Analysis of the droplet film boiling heat transfer under ambient pressure*. Proceedings of 3rd Int. Conf. on Contemporary Problems of Thermal Engineering, CPOTE 2012, 18-20. ISBN 978-83-61506-13-3.

Orzechowski, T. (2021). Peculiarities in Leidenfrost water droplet evaporation. *Heat and Mass Transfer*, *57*, 2021, 529-541. https://doi.org/10.1007/s00231-020-02967-x

Orzechowski, T., Wciślik, S. (2014). Instantaneous heat transfer for large droplets levitating over a hot surface. *Int. J. Heat and Mass Transfer*, *73*, 110-117. https://doi.org/10.1016/j.ijheatmasstransfer.2014.02.008

Pastuszko, R., Kaniowski, R., Dadas, N., Bedla-Pawlusek, M. (2021). Pool boiling enhancement and a method of bubble diameter determination on surfaces with deep minichannels. *International Journal of Heat and Mass Transfer*, *179*, 121713, ISSN 0017-9310. https://doi.org/10.1016/j.ijheatmasstransfer.2021.121713

Paul, G, Das, P.K, Manna, I. (2015). Droplet oscillation and pattern formation during Leidenfrost phenomenon. *Exp. Thermal Fluid Sci.*, *60*, 346-353.

Poniewski, M., Staniszewski, B. (1981). *O kryzysie wrzenia błonowego – stan wiedzy*. Biuletyn Informacyjny Instytutu Techniki Cieplnej Politechniki Warszawskiej Nr 59, 1-71. (in Polish)

Poniewski, M., Staniszewski, B. (1986). *Experimental and Theoretical Evidences for Dissipative Model of Film Boiling Crisis*. Proc. VIII Int. Heat Transfer Conf., San Francisco, Vol. 4, 2025-2029.

Pavlenko, A.M., Basok, B.I., Avramenko, A.A. (2005). Heat conduction of a multi-layer disperse particle of emulsion. *Heat Transfer Research*, *36*(1-2), 55-61.

Roques-Carmes, T., Domps, A., Marchal, P. et al. (2018). Equivalent capacitive thickness of the vapor layer below Leidenfrost drops. *Exp Fluids*, *59*, 115. https://doi.org/10.1007/s00348-018-2567-3

Snoeijer, J.H., Brunet, P., Eggers, J. (2009). Maximum size of drops levitated by an air cushion. *Phys. Rev. E*, *79*, 036307. https://doi.org/10.1103/PhysRevE.79.036307

Sodtke, C., Ajaev, V.S., Stephan, P. (2007). Evaporation of thin liquid droplets on heated surfaces. *Heat Mass Transfer*, *43*, 649-657. https://doi.org/10.1007/s00231-006-0126-6

Wciślik, S., Mukherjee, S. (2022). Evaluation of three methods of static contact angle measurements for $TiO_2$ nanofluid droplets during evaporation. *Phys. Fluids*, *34*, 062006. https://doi.org/10.1063/5.0096644